Excited-state absorption of excitons confined in spherical quantum dots

T. Uozumi and Y. Kayanuma
College of Engineering, Osaka Prefecture University, Sakai 599-8531, Japan

K. Yamanaka, K. Edamatsu, and T. Itoh
Graduate School of Engineering Science, Osaka University, Toyonaka 560-8531, Japan

(Received 6 October 1998)

The excited-state photoabsorption spectrum by an electron and a hole confined in spherical quantum dots is calculated. As the dot size is reduced, the calculated absorption peak shifts to the high-energy side, and splits into two peaks in the limit of strong confinement. This splitting represents the changeover of the quantum size effect of the zero-dimensional excitons. Our theoretical result is in agreement with experimental data for the transient infrared absorption spectra under size-selective excitation observed for CuCl nanocrystals embedded in NaCl crystals. [S0163-1829(99)07415-9]

The optical properties of semiconductor quantum dots (QD's) have attracted much interest in recent years.[1] For the most part, attention has been focused on the dramatic modification experienced by the quantum state of the electron-hole (exciton) system due to the zero-dimensional nature of QD's. Recent advances in material growth and optical measurement techniques allow for the observation of optical responses of an assembly of QD's with a very narrow size distribution dispersion,[2] or even of a single QD.[3] It is expected that the concentration of the oscillator strengths in essentially discretized energy levels in QD's will be utilized in the optical device technology.[4] From the theoretical side, this poses an interesting problem involving a few-body system, namely that of determining the electronic structure of interacting electron-hole pair confined in nanocrystals. A number of theoretical works have been carried out on this subject from various viewpoints.[5–14] Among these, a model of a spherical QD with an effective-mass approximation[5–9,11,13] has been widely used to gain insight into the essential features of quantum size effects. It is well established that there are two extreme situations, characterized by the ratio of the radius R of the QD to the effective Bohr radius a_B^* of the exciton; namely, the regime of exciton confinement, in which $R/a_B^* \gtrsim 4$, and the regime of individual particle confinement, in which $R/a_B^* \lesssim 2$.[8]

CuCl nanocrystals are usually considered as belonging to the exciton confinement regime. Their optical properties have been studied extensively from various viewpoints.[15–18] Most of these studies are, however, concerned with transitions between the ground state and excited states, although some data on infrared absorption under band-to-band excitation[19] and two-photon excitation spectra[20] have also been reported. Recently, Yamanaka *et al.*[21] performed measurements of the transient infrared absorption spectra of CuCl QD's embedded in NaCl crystals under the size-selective direct excitation of the lowest excitons. The obtained spectra exhibit a characteristic dependence on the dot-size: The peak position of the infrared absorption gradually shifts toward the high-energy side as the dotsize is reduced, and the absorption band becomes broadened for the smallest size observed.

The transient absorption spectrum is of special interest, because it contains detailed information on the structure of the excited states that cannot be obtained by studying the spectrum involving only direct absorption from the ground state. In materials such as CuCl that possess a direct energy gap for allowed transitions, the final state resulting from the optical absorption by the ground state can be regarded as an electron-hole state with the envelope function of S-like symmetry if the QD is approximately spherical in shape. Transient infrared absorption at low temperature occurs from the lowest S-like state of the confined electron-hole system. Then, the final state resulting from the absorption should have P symmetry, since the optical process in this case is an intraband transition, implying that the electromagnetic fields act on the envelope function.

Most theoretical works carried out to this time have been devoted to the analysis of the S-like excited state of QD's, while the wave functions of only a few low-lying excited states with higher angular momenta have been calculated.[22] In the present paper, we show results of a theoretical analysis of the excited-state absorption spectra with a systematic investigation of the quantum states of the confined electron and hole in the cases in which the envelope function posseses S-like and P-like symmetry.

Consider a spherical QD with radius R. Within the effective-mass approximation, the Hamiltonian is simply

$$H = \frac{\vec{p}_e^{\,2}}{2m_e} + \frac{\vec{p}_h^{\,2}}{2m_h} - \frac{e^2}{\kappa|\vec{r}_e - \vec{r}_h|}, \tag{1}$$

where $\vec{r}_i$, $\vec{p}_i$ and m_i are the position, the momentum and the effective-mass of the electron ($i=e$) and the hole ($i=h$), and κ is the dielectric constant. We assume complete confinement for the electron and the hole, which requires that the wave function vanishes at $|\vec{r}_e| = R$ and $|\vec{r}_h| = R$. Because of the spherical symmetry of the system, the eigenstates of H can be completely classified in terms of the total angular momentum L, its z component L_z, and one additional quantum number.[23] It is convenient to employ the Hylleraas coordinate system[24] and divide the six degrees of freedom into

two groups, represented by the ''inner'' coordinates and the ''outer'' coordinates. The three inner coordinates can be chosen as $r_e \equiv |\vec{r}_e|$, $r_h \equiv |\vec{r}_h|$, and $r_{eh} \equiv |\vec{r}_e - \vec{r}_h|$. The outer coordinates are chosen as the three Euler angles that determine the plane spanned by the vectors $\vec{r}_e$ and $\vec{r}_h$ at the origin. The outer coordinates are then separated out, and the Schrödinger equation is reduced to that involving only the inner coordinates.

Herafter, we adopt the effective Bohr radius $a_B^* \equiv \kappa\hbar^2/\mu e^2$ as the unit of length and the effective Rydberg energy $E_{Ry}^* \equiv \hbar^2/2\mu a_B^{*2}$ as the unit of energy (μ is the reduced mass). In the *S*-like subspace ($L=0$), the wave function depends only on the inner coordinates, and the effective Hamiltonian is[7]

$$H_0 = -\frac{c_e}{r_e^2}\frac{\partial}{\partial r_e}\left(r_e^2\frac{\partial}{\partial r_e}\right) - \frac{c_h}{r_h^2}\frac{\partial}{\partial r_h}\left(r_h^2\frac{\partial}{\partial r_h}\right) - \left(\frac{c_e}{r_e^2}+\frac{c_h}{r_h^2}\right)\frac{1}{\sin\theta}\frac{\partial}{\partial\theta}\left(\sin\theta\frac{\partial}{\partial\theta}\right) - \frac{2}{r_{eh}}, \quad (2)$$

where θ is the angle between $\vec{r}_e$ and $\vec{r}_h$ defined by $r_{eh}^2 = r_e^2 + r_h^2 - 2r_e r_h\cos\theta$, and c_e and c_h are defined in terms of the effective mass ratio $\sigma \equiv m_h/m_e$ as $c_e \equiv \sigma/(1+\sigma)$ and $c_h \equiv 1/(1+\sigma)$. For the subspace of *P* symmetry, we extend the formalism developed by Breit[25] for the excited states of He atoms to the electron-hole system. The subspace of *P*-symmetry ($L=1$) itself is further divided into two subspaces according to parity. These subspaces are denoted P^+ and P^-. From the lowest S^+ state, only transitions to the subspace P^- are optically allowed. The states belonging to P^+ are optically inactive in one-photon transitions both from the ground state and from the lowest excited *S* state. The details of the energy scheme for each subspace will be presented elsewhere. In the remainder of the paper, we concentrate on the P^- subspace.

Without loss of generality, we assume that the electric field of the infrared radiation is *z* polarized, and we restrict ourselves to states with $L=1$ and $L_z=0$ of odd parity. The wave function in this subspace is written[25]

$$\psi(\vec{r}_e,\vec{r}_h) = f_1(r_e,r_h,r_{eh})\cos\theta' + f_2(r_e,r_h,r_{eh})\sin\theta'\cos\phi, \quad (3)$$

where θ' is the polar angle of the electron and ϕ is the angle between the plane spanned by the *z* axis and $\vec{r}_e$ and that spanned by $\vec{r}_e$ and $\vec{r}_h$. Essentially the same wave function has been used in Ref. 22. The Euler angles θ', ϕ and ϕ' (the azimuthal angle of the electron) can be removed from the Schrödinger equation, and we obtain a set of simultaneous equations,

$$\sum_{j=1}^{2} H_{ij} f_j(r_e,r_h,r_{eh}) = E f_i(r_e,r_h,r_{eh}), \quad (i=1,2), \quad (4)$$

for the eigenvalue *E*. Here, the effective Hamiltonians H_{ij} are given by

$$H_{11} = H_0 + \frac{2c_e}{r_e^2}, \quad (5)$$

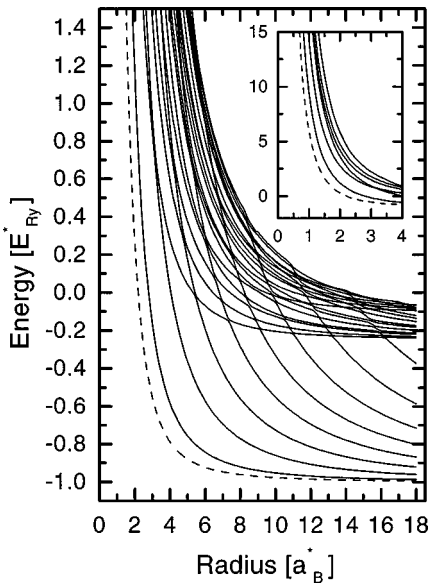

FIG. 1. Calculated energy levels of an electron-hole pair in a spherical quantum dot with P^- symmetry (solid lines). Only the lowest 24 states are plotted for the mass ratio $\sigma=3$. The lowest energy level with S^+ symmetry is represented by the dashed line. The energy levels for low-lying states in the strong confinement region are shown in the inset.

$$H_{22} = H_0 + \frac{1}{\sin^2\theta}\left(\frac{c_e}{r_e^2}+\frac{c_h}{r_h^2}\right), \quad (6)$$

$$H_{12} = \frac{2c_e}{r_e^2}\left(\cot\theta + \frac{\partial}{\partial\theta}\right), \quad (7)$$

$$H_{21} = -\frac{2c_e}{r_e^2}\frac{\partial}{\partial\theta}. \quad (8)$$

Equation (4) can be solved numerically by transforming it into an eigenvalue problem for the Hamiltonian matrix by expanding $f_i(r_e,r_h,r_{eh})$ in a series composed of a complete set of orthonormal basis functions satisfying the boundary conditions. In the actual calculation, it is crucial to adopt basis functions which incorporate the electron-hole correlation from the beginning. We use the orthogonalized linear combination of the correlated basis set,[8] $\varphi_m(r_e/R)\varphi_n(r_h/R)r_{eh}^l\exp(-\alpha r_{eh})$, ($l=0,1,2,\cdots$; $m,\ n=1,2,3,\cdots$), where φ_m is the $2m$th order polynomial defined by the Legendre polynomials, $\varphi_m(x) = P_{2m-1}(x)(1-x^2)/x$, and α is a variational parameter, which is adjusted to minimize the lowest eigen-energy.

The solid lines in Fig. 1 represent calculated energy levels for the confined electron-hole system with P^- symmetry with $\sigma=3$ as a function of the normalized radius of the QD. In the calculation, 250 basis functions were used and only the lowest 24 levels are plotted here. The lowest energy state with *S* symmetry, which is the initial state of the transition, is represented by the dashed line. We note that, in the weak-confinement region $R/a_B^* \gtrsim 4$, the energy scheme reflects the separation of the motional degrees of freedom into the center-of-mass motion of the exciton and the relative motion of the electron and hole. The exciton Rydberg states with principal quantum numbers 1, 2, and 3 are clearly observed.

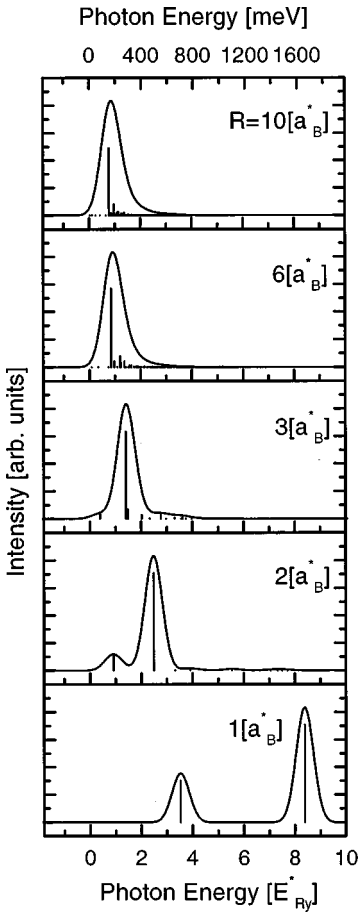

FIG. 2. Calculated transient absorption spectra of the confined electron-hole pair with $\sigma=3$ for various quantum dot radii. In the upper axis, the energy units for CuCl ($E^*_{Ry}\simeq 197$ meV) are shown. The intensities of the spectra have been normalized so that they are the same at their peak positions.

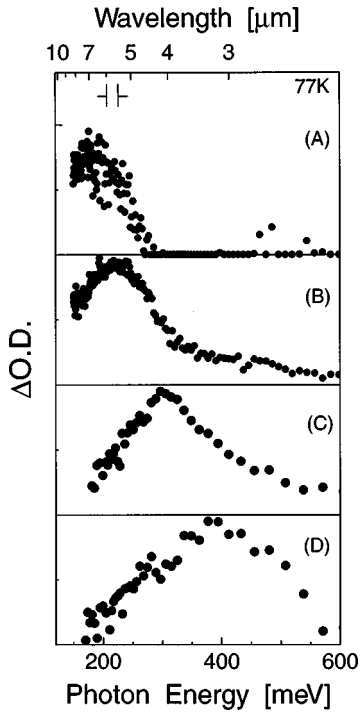

FIG. 3. The observed transient absorption spectra for CuCl nanocrystals embedded in NaCl crystals at $T=77$ K. The radii R of the CuCl nanocrystals for (a)-(d) are estimated as $\geqslant$10.5, 5.8, 2.3, and 1.8 nm, respectively, using the energy formula for exciton confinement (Refs. 5 and 8) with a dead-layer width $a^*_B/2$. The intensities of the spectra have been normalized so that they are the same at their peak positions.

The lower energy states correspond to the exciton $1s$ state with the nP center-of-mass motional state ($n=1,2,3,\ldots$) of the confinement. We denote these states as $(1s,nP)$. Higher energy states are denoted as $(2p,nS)$, $(2p,nD)$, $(2s,nP)$, and so on. Of course, this separation is not complete since the relative motion and the center-of-mass motion are coupled through the boundary conditions at the spherical surface. However, the magnitudes of level repulsions between states with different principal quantum numbers, $(1s,nP)$ and $(2p,n'S)$ for example, at the avoided crossings are quite small (typically of order of $0.03E^*_{Ry}$ for $R/a^*_B\simeq 10$). Thus, the picture of the ''confinement of the exciton'' works fairly well in the weak-confinement region. As we enter the region of strong confinement $R/a^*_B\lesssim 2$, the notion of the exciton as a *quasiparticle* loses its meaning, and here the eigenstates should be labeled by the quantum numbers of the individually confined electron and hole as $(np_e,n's_h)$, $(ns_e,n'p_h)$, $(np_e,n'd_h)(n,n'=1,2,3,\ldots)$. The level scheme and the transient absorption spectrum depend strongly on the mass ratio σ in this region.

Figure 2 diplays the calculated size-dependence of the excited-state absorption spectrum for $\sigma=3$. The continuous spectra were obtained by convoluting the line spectra with a Gaussian function of width $0.4E^*_{Ry}$ half width at half maximum. In the weak-confinement region, the main line corresponds to the internal transition of the exciton from the $(1s,1S)$ state to the $(2p,1S)$ state. The high-energy absorption lines correspond to the transitions to $(np,1S)(n\geqslant 3)$, which are mixed with other states. The very weak absorption lines at the low-energy side of the main line correspond to excitations of the center-of-mass motion, $(1s,1S)\rightarrow(1s,nP)(n\geqslant 1)$. Transfer of the oscillator strength to these states is induced by the breaking of the translational symmetry. As the radius R becomes smaller, the main line exhibits a moderate blueshift, indicating that the high-energy shift of the $(2p,1S)$ state is larger than that of $(1s,1S)$ state. This is essentially due to the fact that the $2p$ exciton has a radius twice or three times as large as that of the $1s$ exciton. It is pointed out in Ref. 8 that the free volume of a QD is effectively reduced by the dead-layer effect of the exciton. In the region $R/a^*_B\lesssim 2$, the spectrum suffers a drastic change. The lowest P^- state gains intensity, and the entire line shape comes to display a double-peak structure. The lower peak corresponds to the transition $(1s_e,1s_h)\rightarrow(1s_e,1p_h)$ and the higher one to $(1s_e,1s_h)\rightarrow(1p_e,1s_h)$ in the $\sigma>1$ case. We, thus, see that the dipole moment $\vec{M}\equiv -e\vec{r}_{eh}=e\vec{r}_h-e\vec{r}_e$ for optical transition induces the internal polarization of the exciton with respect to the center-of-mass in the weak-confinement region, while it gives rise to the individual polarization of the electron and the hole with respect to the center of the QD in the strong confinement region. This changeover most clearly reflects the size-dependent transformation of the motional states of the electron-hole pair and the way it responds to external fields.

In Fig. 3, observed spectra of infrared absorption for CuCl nanocrystals in NaCl (Ref. 21) under size-selective excitations are shown. The parameter values for CuCl have been estimated as[21] $\sigma \simeq 3$, $a_B^* \simeq 0.7$ nm, $E_{Ry}^* \simeq 197$ meV. Although the experimental data display a dispersion partly due to inhomogeneity of crystals and partly due to instrumental broadening, a gradual increase of the peak energy with the reduction of the dot size is clearly seen. The agreement between the observed spectral features and the theoretical calculation is good, not only qualitatively but also quantitatively. Thus we conclude that the size-dependent blue-shift of the transient absorption spectra reflects the dependence of the quantum size effect on the internal excitation. The anomalous broadening of the spectrum for the smallest size of dots ($R/a_B^* \simeq 2.5$) shown in Fig. 3(d) is interesting. We conjecture that this is due to the unresolved double peak structure, which is an indication that in this case the system is near the region of individual particle confinement, as shown in Fig. 2. Experimental investigation to confirm this point is in progress.

In conclusion, we have presented a systematic analysis of the electronic structure of the excited states of an electron-hole system in QD's. The size-dependent transient absorption spectra observed for CuCl nanocrystals have been reproduced fairly well. The formalism proposed here can readily be extended to still higher angular momentum states. This means that responses to various external perturbations of the QD's can be calculated with a high accuracy. Such a calculations will be carried out in a separate paper. Experimental investigations of the excited-state absorption spectra for QD's of other materials are also desirable.

This work was partially supported by Grants-in-Aid for COE and for Scientific Research from the Ministry of Education, Science, Sports and Culture of Japan and by Research for the Future from the Japan Society for the Promotion of Science.

[1] See, for example, A. D. Yoffe, Adv. Phys. **42**, 173 (1993); U. Waggon, *Optical Properties of Semiconductor Quantum Dots* (Springer, Berlin, 1997), and references therein.
[2] M. G. Bawendi *et al.*, Phys. Rev. Lett. **65**, 1623 (1990).
[3] M. Nirmal *et al.*, Nature (London) **383**, 802 (1996); M. Grundmann *et al.*, Phys. Rev. Lett. **74**, 4043 (1995).
[4] Y. Arakawa and H. Sakaki, Appl. Phys. Lett. **40**, 939 (1982).
[5] Al. L. Efros and A. L. Efros, Fiz. Tekh. Poluprovdn. **16**. 1209 (1982) [Sov. Phys. Semicond. **16**, 772 (1982)].
[6] L. E. Brus, J. Chem. Phys. **80**, 4403 (1984).
[7] Y. Kayanuma, Solid State Commun. **59**, 405 (1986).
[8] Y. Kayanuma, Phys. Rev. B **38**, 9797 (1988).
[9] T. Takagahara, Phys. Rev. B **39**, 10 206 (1989).
[10] P. E. Lippens and M. Lannoo, Phys. Rev. B **39**, 10 935 (1989).
[11] Y. Z. Hu, M. Lindberg, and S. W. Koch, Phys. Rev. B **42**, 1713 (1990).
[12] M. V. Rama Krishna and R. A. Friesner, Phys. Rev. Lett. **67**, 629 (1991).
[13] G. T. Einevoll, Phys. Rev. B **45**, 3410 (1992).
[14] N. A. Hill and K. B. Whaley, J. Chem. Phys. **100**, 2831 (1993).
[15] A. I. Ekimov, Al. L. Efros, and A. A. Onushchenko, Solid State Commun. **56**, 921 (1985).
[16] T. Itoh, Y. Iwabuchi, and M. Kataoka, Phys. Status Solidi B **145**, 567 (1988).
[17] K. Edamatsu, J. Lumin. **70**, 377 (1996).
[18] Y. Masumoto, J. Lumin. **70**, 386 (1996).
[19] Y. Miura, K. Edamatsu, and T. Itoh, J. Lumin. **66&67**, 401 (1996).
[20] K. Edamatsu, K. Hisakawa, and T. Itoh, J. Lumin. **72/74**, 329 (1997).
[21] K. Yamanaka, K. Edamatsu, and T. Itoh, J. Lumin. **76&77**, 256 (1998).
[22] S. V. Nair and T. Takagahara, Phys. Rev. B **53**, R10 516 (1996).
[23] See, for instance, M. Morse and H. Feshbach, *Method of Theoretical Physics* (McGraw-Hill, New York, 1953), p. 1721.
[24] E. A. Hylleraas, Z. Phys. **54**, 347 (1929).
[25] G. Breit, Phys. Rev. **35**, 569 (1930).